Towards an Untethered Knit Fabric Soft Continuum Robotic Module with Embedded Fabric Sensing

Pham H. Nguyen, *Student Member, IEEE*, Zhi Qiao, *Student Member, IEEE*, Sam Seidel, Sunny Amatya, *Student Member, IEEE*, Imran I. B. Mohd, and Wenlong Zhang*, *Member, IEEE*

***Abstract*— In this paper, we present the design and testing of a continuum, lightweight, multi-degree of freedom (DOF) soft robotic module made of high-stretch knit fabric. A set of design criteria, inspired by muscular hydrostats found in elephant trunks, is presented in order to create a highly articulated and robust soft robotic module. The soft continuum robotic module can vertically extend and twist along its central axis, as well as bend in 3D space. The material properties of the knit fabrics are characterized. The bending articulation and payload capabilities of the module are investigated. This work also demonstrates the embedded integration of a thin, flexible, and conductive fabric stretch sensor with the module to provide pose information for motion tracking. An on-board electropnuematic system is also developed. This system allows for the future creation of safe human-robot interfaces that are multi-functional integration of multiple soft robotic modular units that are deployable for various complex tasks.**

I. INTRODUCTION

With the interests in soft robotics on the rise, there have been extensive studies of soft materials, actuation, control, sensing, and even soft pneumatic pumps and valves [1], [2]. Soft robotic systems have shown advantages of being lightweight, highly compliant, articulate, and inherently safe for interactions with human body and environment. Thus, soft robotic systems have been developed for diverse applications such as locomotion in unstructured environments [2], manipulation of objects with various sizes and shapes [3], invasive surgical instruments [4], and assistive/rehabilitative devices [5], [6].

Soft continuum robots are popular in manufacturing and surgical tasks as well as activities of daily living (ADL) [1], [7]. Such robots have been created by combining various types of soft actuation mechanisms, including cable-driven systems [8], [9], pneumatic artificial muscles (PAMs) [10], and inflatable actuators made of elastomers [11]–[13], origami [14], [15], fabric [16]–[18], and combination of materials [19]. Our recent work has shown versatility and promise in applying elastomeric and woven fabric actuators to build soft continuum robotic arms that are robust, lightweight, and compliant enough to assist with ADL tasks [12], [17].

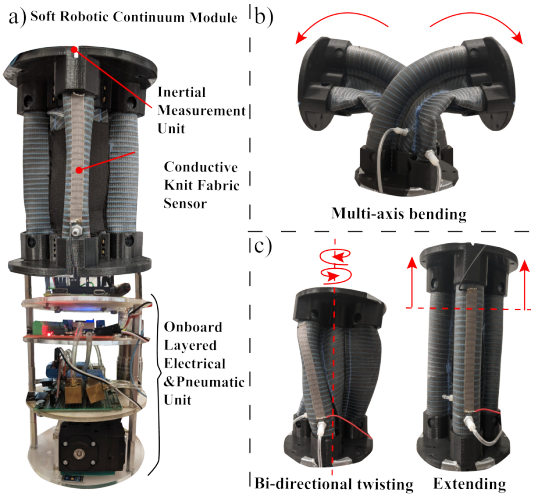

Fig. 1: (a) The developed soft continuum robotic module. (b) The soft module performing mutli-axis bending. (c) The soft module performing bi-directional twisting (left) and linear extension (right).

However, our previous developments have been confined to a fixed setting because of the tethered pneumatic source and pose sensing using a motion capture system [12], [17]. For portable pneumatic systems, there have been studies on the use of pneumatic cylinders, compressed air supplies, and storage tanks to power soft robots [13], [20]. In order to develop compact soft robots that are modular and deployable in outdoor applications or used as educational toolkits [19], [21], the aforementioned portable pneumatic systems can be more bulky than necessary. In this work, we aim to add we aim to add a compact off-board electropneumatic system to control the soft robotic module.

With high degree-of-freedom (DOF) continuum robots working and interacting with the environment, there is a need to monitor the compliant and highly deformable nature of the soft robot in order to understand its locomotion capabilities as well as the inherent contact with obstacles. Thus, proprioception and tactile feedback are essential in controlling the movement of high-DOF continuum robots. To satisfy these needs, different types of soft sensors have been developed, such as textile electrode-based, liquid metal-based, nanocomposite-based, optical-fiber based, and conductive yarn-based sensors [22]–[27].

In this work, we present a robust, compact, lightweight, and highly articulated soft robotic module, inspired by hydrostatic muscles. This work highlights the first soft continuum

This work was supported in part by the National Science Foundation under Grant CMMI-1800940.

P. Nguyen, S. Seidel, S. Amatya, and W. Zhang are with the Polytechnic School, Ira A. Fulton Schools of Engineering, Arizona State University, Mesa, AZ 85212, USA. {nhpham2, shseidel, samatya, wenlong.zhang}@asu.edu

Z. Qiao and I. Mohd are with School for Engineering of Matter, Transport and Energy, Ira A. Fulton Schools of Engineering, Arizona State University, Tempe, AZ 85281, USA. {zhi.qiao.1, imohd}@asu.edu

∗ Address all correspondence to this author.

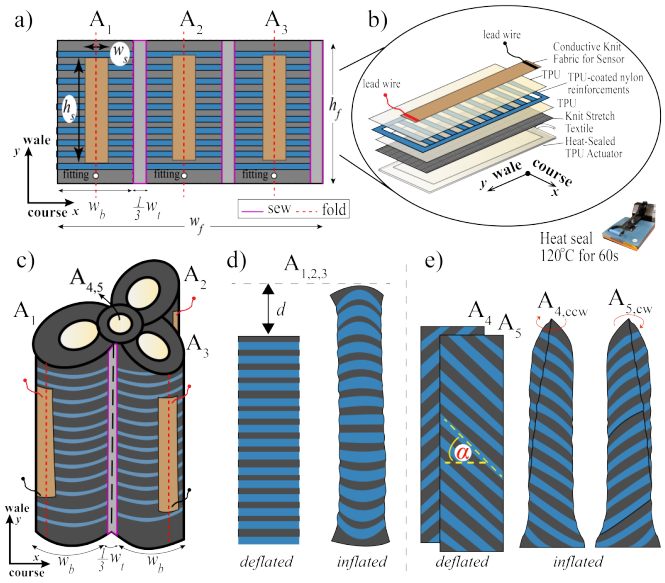

Fig. 2: Fabrication scheme of the soft continuum robotic module. a)The fabrication layout to create the module in just using folding and sewing. b) The single step actuator fabrication method for multi-layer fabrics, to include both embedded sensing and actuation. c) Final product after folding and sewing the actuator together. $A_{1,2,3}$ are the extending actuators and $A_{4,5}$ are the central twisting actuators. d) $A_{1,2,3}$ are the extending actuators ($w_b = 80mm$, $h_f = 180mm$, and $\alpha = 0°$) e) $A_{4,5}$ are the central twisting actuators that can twist clockwise and counterclockwise ($w_t = 80mm$, $h_f = 180mm$, and $\alpha = \pm 30°$).

robot fabricated using stretch fabric, which can not only bend in 3D space, but also vertically extend and bi-directionally twist. Folding and precision multi-layering fabrication techniques are introduced for low-cost and rapid manufacturing of the actuator. The system utilizes the concept of fabric-reinforced textile actuators (FRTAs) presented in our previous work, made of high-strength and high-stretch knit inflatable fabrics [28].

In addition to the actuator design, we also demonstrate the integration of a highly stretchable, conductive knit-fabric strain sensor on the soft module. Because of the sensor's high stretchability, it is able to obtain sensory feedback for state estimation of the knit fabric actuators, while still allowing the actuators to maintain its hyperelastic nature. Furthermore, the module contains on-board electropnuematic hardware, wireless communication, and additional IMU sensors attached to the actuator. The all-inclusive on-board system allows for communication, computation, distributed sensing, actuation, and control as a first step to extend it into real-world applications.

The remainder of the paper is organized as follows. Section II introduces the design, material characterization, and fabrication process of the robotic module. Section III presents the on-board electropneumatic system. The sensor characterization of the soft sensing module is presetned in Section IV. Section V evaluates the payload and motion capabilities of the soft module, and preliminary motion tracking using IMU and the soft fabric sensors. Section VI concludes this paper and discusses future directions.

II. Design and Fabrication

As seen in biology, muscular hydrostats are found in elephant trunks and octopus arms, which contain muscles or fibers that are oriented longitudinally, circumferentially, radially and/or transversely. When working in tandem with one another, these fibers enable elongating, shortening, and bending motions, while helically arranged fibers create axial torsion or twisting. Inspired by biology, we develop a soft continuum robotic module that performs active multi-axis bending, twisting, and extending all within one actuation module. Each module includes three extending FRTAs for multi-directional bending and linear elongation, and two twisting actuators for bi-directional twisting and counteracting torsional disturbances, as seen in Fig. 2d) and e). The size of each soft continuum robotic module is determined so that three modules can eventually be connected in series to a create a full-length soft continuum robotic arm, which matches the length of an average sized male arm ($0.59m$) [12]. We also utilize highly stretchable conductive knit fabric sensors, embedded onto the skin of the knit material, to measure the strain of the FRTAs during elongation and bending.

A. Material Selection

In this work, we selected a bi-directional high-stretch knit material, the COTOWIN Heavy Stretch Elastic Band (Amazon.com Inc., Seattle, WA), with a density of $850.3kg/m^3$. We tested the inflatable fabric using a burst test, to find out the maximum pressure that the fabrics could withstand before failure, using the ASTM F2054 protocol. Each actuator had the same fabric-reinforcement arrangement along the surface. The selected material for the fabric-reinforcements is a 200D TPU-coated nylon fabric (6607, Rockywoods Fabric, Loveland, CO), with a density of $840kg/m^3$. The inflatable actuator is able to withstand the set maximum safety pressure of $0.69MPa$ without bursting, thus showing high robustness and the capability of achieving increased payload.

We characterize the material properties of the COTOWIN Heavy Stretch Elastic Band material using the ISO-139134-1 standard, where the material is stretched both in the wale and course directions, using a universal testing machine (UTM) (Instron 5944, Instron Corp., High Wycombe, United Kingdom). The material is tested both with and without the fabric-reinforcements. For the fabrics without reinforcements, in the wale direction (y-direction), parallel to the direction of manufacturing, the fabric had a stretch of 204.94% at $8.84MPa$. In the course direction (x-direction), perpendicular to the direction of manufacturing, the stretch was much stiffer at 12.3% at $32.8MPa$, exceeding the payload set by the universal testing machine of $1kN$ without tearing. The fabrics with reinforcements showed an increase of overall stiffness but maintaining similar properties of the textiles at 218.77% at $8.544MPa$ (in the wale direction) and 11% at $32.8MPa$ (in the course direction), respectively. The material properties of the conductive knit fabric (A321, LessEMF, Latham, NY) used for the strain sensor, had a stretch of 272.65%, in the wale direction and 175.52%, in the course direction. The material properties of the woven TPU-coated

Nylon (6607, Rockywoods Fabric, CO), which was used as fabric-reinforcements, were determined with a linear elastic modulus: Young's modulus of $E = 498MPa$ and Poisson's ratio of $v = 0.35$ [17].

B. Fabrication and Integration

To fabricate the soft continuum robotic module with embedded sensors, the fabrics are cut into the shape specifications using a laser cutter (Glowforge Prof, Glowforge, Seattle, WA). The different layer of fabrics, as seen in Fig. 2b), are precisely aligned, from top-view, as seen in Fig. 2a). The heat press (FLHP 3802, FancierStudio, Hayward, CA) is used to laminate the sensor fabric, the fabric reinforcement, and the knit base fabric layers together. The widths of the extending and twisting actuators are defined by w_b and w_t, respectively. The laminated layered fabric in Fig. 2a), is folded along the red dashed line, and sewn using high-stretch elastic thread (Maxi Lock Stretch, American & Efird, Mount Holly, NC) along the pink lines, to create the 3D structure seen in Fig. 2c). The sensing materials are aligned at the center of the fold lines to measure where the actuator extends the most. $A_{1,2,3}$ represent the three extending actuators that inflate and extend upon pressurization, as seen in Fig. 2d). Due to the centralized strain-limiting layer created by the pink sewn lines seen in Fig. 2a and c), the actuators, $A_{1,2,3}$, will bend when inflated separately or in pairs, but will extend when all three are inflated together.

The bi-directional twisting actuators ($A_{4,5}$) are manufactured separately [28] and added to the stem of the soft continuum robotic module as shown in Fig. 2c). For the twisting actuators, the fabric reinforcements are angled at the desired twisting angle α = 30° for counterclockwise motion (actuator A_4) and α = -30° for clockwise motion (actuator A_5), as seen in Fig. 2e). Because of the high collapsibility and almost zero initial stiffness of fabrics, two twisting actuators are able to fit within the central space of the actuator (as seen in Fig. 2c), allowing for a compact design of the bidirectional twisting actuators. The width of the extending and twisting actuators are defined by w_b and w_t. correspondingly.

III. Electronics and Hardware

The design of embedded hardware aims at allowing independent sensing and control of each soft robotic module. To this end, a four-layered system is encased within a cylindrical box (radius=60mm, height=140mm), as seen in Fig. 1. As shown in Fig. 33a), the control unit is designed using off-the-shelf components to regulate pressure in the five actuators output lines. A miniature pump (NMP830 HP,KNF Neuberger, Inc., Trenton, NJ) is used to generate up to 0.19MPa of source pressure. The airflow of the unit is controlled by one proportional valve (Enfield Technologies, Shelton, CT), and five 3/2-Way solenoid valves (Miniature Solenoid Valve, Parker Hannifin, Hollis, NH). The inflation and deflation processes for each actuator are measured by a pressure sensor (ABPMANN004PGAA5, Honeywell International Inc., Morris Plains, NJ). The orientation of the end-effector is measured by a 9-DOF inertia measurement unit (IMU) (Adafruit BNO055 Board, Adafruit Industries, New York, NY). In this work, the IMU sensor is specifically utilized for measuring twisting and bending. The microcontroller (Raspberry Pi Zero W, Raspberry Pi Foundation, United Kingdom) controls the pump, valves, pressure and IMU sensor on the module. It contains an on-board Wi-Fi module, allowing a wireless TCP/IP communication between the module and the central PC for sending the desired pressure commands, as well as pressure and sensing measurements. This communication can be extended to inter-module communication if necessary. The overview of the system is depicted in Fig. 3b).

IV. Embedded Sensing

In this section, we characterize the embedded knit stretch sensor, aligned with the three extending-bending actuators along the length of the actuator. When the soft module bends, we assume variable constant curvature to model the system [29]. The lengths of the three extending-bending actuators $[s_1, s_2, s_3]$ are estimated by their corresponding resistance sensor values $[R_1, R_2, R_3]$. The arc parameters of the module are defined in Fig. 6 and the arc length of the central axis of the module S is calculated as described in Wurderman et al. [24] and Webster et al. [29].

A. Sensor Selection and Characterization

In order to characterize the embedded soft fabric sensor we placed the sensorized fabric on the UTM to perform loading and unloading tests for ten cycles. To detect the resistance changes in the conductive knit stretch sensor, a customized

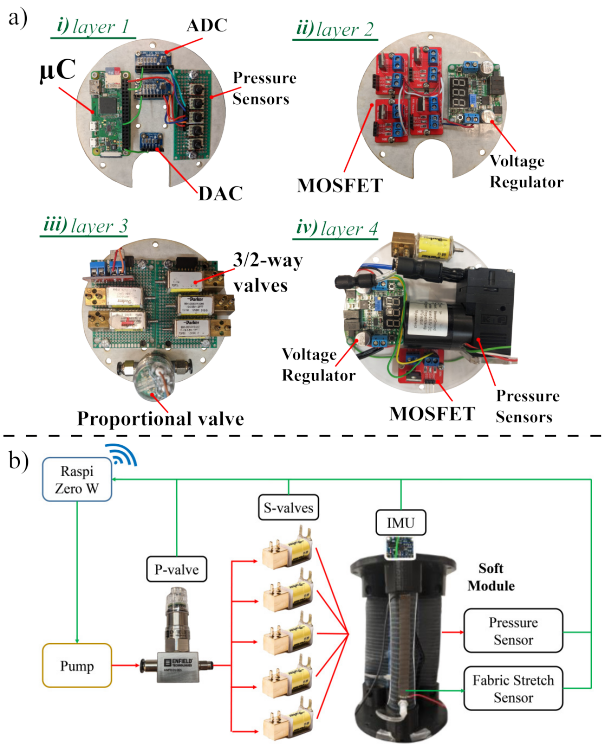

Fig. 3: a) Layered control and actuation system. b) System control flow diagram

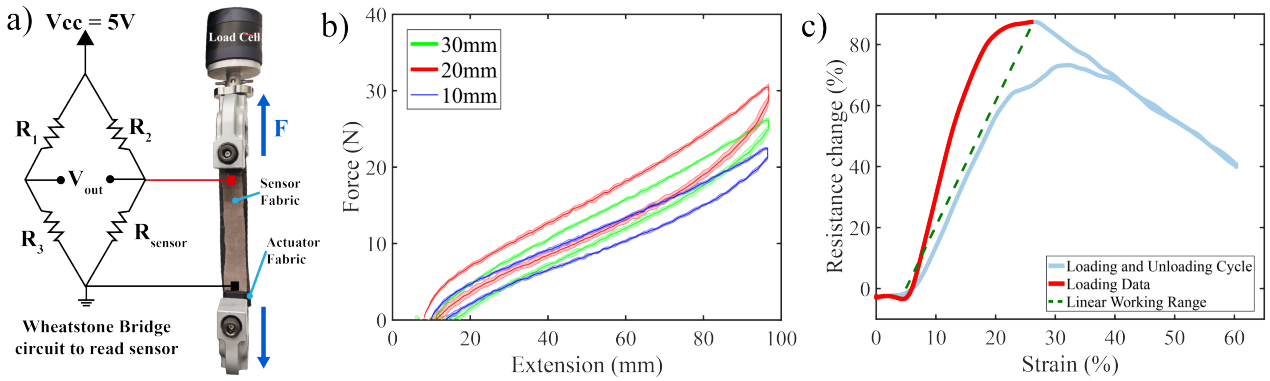

Fig. 4: Sensor setup and characterization. a) UTM sensor characterization setup. b) Hysteresis comparison between three sensor widths of 10*mm*, 20*mm*, and 30*mm*. c) Working range for an average of 10 cycles for the sensor with a 10*mm* width

Wheatstone bridge circuit was used, as shown in Fig. 4a). The first strain cycle was not included in the data analysis to remove any Mullins effect. The strain rate was $96mm/min$ based on the actuator's inflation rate to reach the desired bending angle of 90°. We defined the length of the sensor based on the length of the actuator (165*mm*).

The force-extension behaviors of the sensor for different widths were calculated by varying the width along the fold of the actuator to be: 10*mm*, 20*mm*, and 30*mm*. As seen in Fig. 4b), the sensors show the maximal hysteresis values of 12.04*N*, 14.87*N* and 13.73*N* at 60% strain, for 10*mm*, 20*mm* and 30*mm* width, respectively. The 10*mm* width sensor shows a higher sensing range and lower hysteresis in comparison. The material has a high stretch-to-relax time of 1.5*s* and 0*s* for loading and unloading [30]. The working range of the 10*mm* width sensor was maximized at 26.34% strain and then the resistance begins to decrease for higher strain values, as seen in Fig. 4c). This relationship is due to the specific nature of the multi-material combination of the fabric sensor [30]. Finally, the strain-resistance linear characteristic of the 10*mm* sensor is shown in Fig. 4c). The results show that the fabric sensor's resistance was proportional to the strain within its working range, where the coefficient of the determination using linear regression was $R^2 = 0.953$. The gauge factor (GF) was also calculated within the linear range to be approximately 3.92, comparable to previous LessEMF conductive fabrics [30]. A high GF value means the sensor has higher sensitivity and is able to detect small changes in strain.

V. Testing the Soft Continuum Robotic Module

In order to evaluate the capability of the soft continuum robotic module, we characterize the system for its maneuverability and payload capabilities. Finally, the IMU and conductive knit stretch sensors are evaluated for state tracking and closed-loop control.

A. Device Characterization

In order to investigate the load performance of the soft continuum robotic module, we designed three tests for bending, extending, and twisting tasks. All bending and torque payload tests were performed on the UTM and each output was measured at small pressure increments of 0.034*MPa* until a safety pressure of 0.207*MPa* was reached. Each experiment was repeated three times. The performance characteristics of the soft continuum robotic module are highlighted in Tab. I.

1) Bending Payload Capacity: When one side of the actuator was positioned and inflated, the module's maximum bending payload was 10.00±0.27*N*, as seen in Fig. 5. When two adjacent actuators in the module were inflated to the same pressure, the maximum bending payload was noticed to be similar at 9.32±0.12*N*. Therefore, we assume this is comparable to lifting a weight of almost 1*kg* at the actuator length of 0.165*m*.

2) Torsion Torque Capacity: The twisting actuators were inflated, while being connected to the UTM with a string as shown in Fig. 5b). At the maximum pressure, the twisting actuators in the center of the module was capable of generating 0.98±0.01*Nm* with a lever arm of 0.06*m* as seen in Tab. I. By allowing bi-directional twisting, the twisting actuators would be able to counteract any torsion disturbances of up to approximately 1*Nm* at edge of the module.

3) Extension Payload Capacity: In this test, the extension payload capacity was determined by inflating all three actuators at the same pressure, under the UTM, as shown in Fig. 5c). The maximum extension payload capacity was 231.92±0.41*N* at 0.138*MPa* as shown in Tab. I.

B. Range of Motion

To estimate the range of motion (RoM), the soft continuum robotic module was mounted parallel to the ground. Two sets of three passive markers were mounted at the base and top plates. For each plate, position of the center point and rotation angles are recorded by the motion capture (MOCAP) system (Optitrack, NaturalPoint Inc., Corvallis, OR). For linear elongated motion, three extending-bending actuators were inflated and all held at 0.207*MPa*. In the bending test, only a single extending-bending actuator was inflated to 0.207*MPa*. In the unconstrained twisting test, the bi-directional twisting actuator was inflated on its own, without being mounted on the soft continuum robotic module. The constrained twisting test had all the actuators mounted. For both twisting tests, one twisting actuator was inflated up to 0.172*MPa*, while the other one was kept deflated. By inflating the other twisting actuator, the RoM was measured

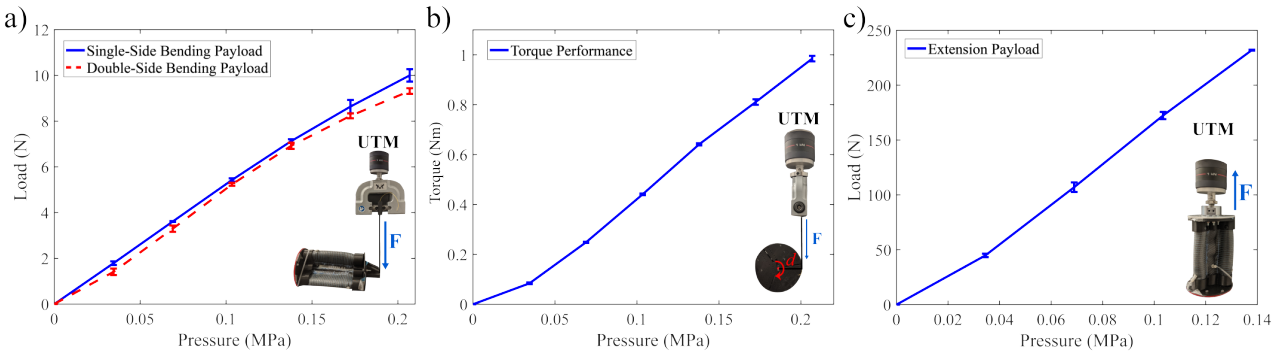

Fig. 5: Payload characterization: a) Bending payload performance. b) Torque performance. c) Extension payload performance

TABLE I: Performance Summary of the Soft Robotic Module

PROPERTY	SPECIFICATION
Single actuator mass	0.03kg
Soft module mass	0.40kg
Electropneumatics' mass	1.076kg
Contracted size	120×120×200 mm
Extended size	120×120×234.38 mm
Linear RoM	34.38 mm
Angular RoM	104.02°
Single actuator torsional RoM	166.70°
Soft module torsional RoM	82.70°
Linear payload	231.92±0.41N
Bending payload	10±0.27N (single side)
	9.32±0.12N (double side)
Torsional performance	0.99±0.01Nm

for twisting motion in clockwise and counterclockwise directions. Each experiment was conducted three times and the averaged results for elongation, bending and twisting are summarized and presented in Tab. I.

C. Motion Tracking with IMU and Embedded Stretch Sensing

A sensorized soft continuum robotic module was used to evaluate the sensing and control performance. An IMU was attached to the center of the top plate and the resistance values were measured by the embedded strain sensor, along the length of the extending-bending actuator.

An experiment was conducted to compare the arc angle (θ) estimated using the IMU and the values obtained from the MOCAP system. The same marker set as described in the Section V-B was utilized for the MOCAP system. One extending-bending actuator was inflated to 0.138MPa and deflated to 0MPa multiple times while the orientation of the end was recorded. As depicted in Fig. 6b), the arc angle estimate obtained using the IMU is fairly accurate with a root mean square error (RMSE) of 1.97° when compared against the measurement from the MOCAP system.

To evaluate the length change estimation of the module, the three extending-bending actuators were inflated to 0.138MPa and deflated to 0MPa cyclically. From Fig. 6c), it can be observed that the change in length of the module can be estimated accurately with an RMSE of 1.19mm when the stretch sensor and MOCAP measurements are compared.

A experiment to measure the twisting angle (ϕ) of the module using both the IMU and the MOCAP was performed. One twisting actuator was inflated to a pressure of 0.138MPa and deflated to 0MPa cyclically. Fig. 6d) shows that the torsion angle of the module can be successfully estimated using the IMU with an RMSE of 4.69°.

VI. Conclusion and Future Work

In this paper, we developed a novel soft continuum robotic module that was robust, compliant, highly articulated by using combinations of fabric-reinforced textile actuators. The soft robotic module was capable of performing 1) multi-DOF bending using the combination of the three extending-bending actuators, 2) bi-directional twisting using twisting actuators in the center of the module, and 3) extending by inflating all the extending-bending actuators. A fabrication scheme was introduced to fabricate the actuators embedded with sensors, by exploiting folding and precision multi-layer fabrication using various 2D manufacturing methods including heat-pressing, sewing, and laser cutting. This fabrication method would, in the future, allow one-step and rapid manufacturing of n number of actuators using just folding and sewing techniques. A larger number of actuators can

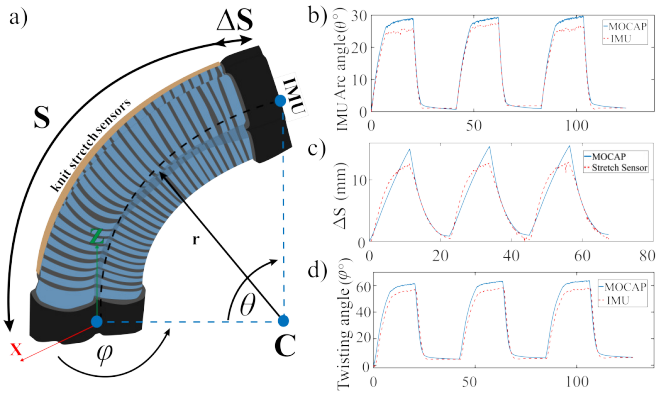

Fig. 6: Motion tracking experiments with embedded sensing. a) The arc parameters of the soft module. S is the arc length of the central axis of the module. r and θ are the bending radius and arc angle ($S = r\theta$), respectively. φ is the orientation of the module A_1. The arc angle and orientation are estimated by the IMU sensor. b) IMU arc angle estimation, bending up to 30° at 0.138MPa. RMSE error is 1.97°. c) Embedded fabric sensor with length change estimation. A five-point moving average filter scheme is used. The actuator elongates up to 15.01mm at 0.138MPa, and the RMSE error is 1.19mm. d) IMU twisting angle estimation, with twisting up to 60° at 0.138MPa and an RMSE error of 4.69°.

further provide higher linear stiffness and payload capacity while being redundant, so it would still be functional even if one or more of the actuators were to fail.

This work also demonstrated the integration of an embedded conductive knit stretch fabric sensor to measure the elongation of each actuator. An additional IMU sensor was used to provide information of the twisting and bending angles of the multi-DOF continuum module. In this work, we also developed an all-inclusive on-board system that included electropneumatics and wireless communication. This on-board system was a first step towards developing a robust, lightweight, fully-integrated soft continuum robotic module.

Analytical and computational models for the soft continuum robotic module will also be created with continuum mechanics and finite element methods, respectively. Future work will also include further developing the embedded sensing scheme in order to determine the central-axis twisting angle of each module. Further studies will also be conducted to study the coupled motion between extension, torsion, and bending. Future efforts will also be made towards distributed sensing and control of multiple modules with communication between neighbors to make the system scalable for different real-world applications.

REFERENCES

[1] D. Rus and M. T. Tolley, "Design, fabrication and control of soft robots," *Nature*, vol. 521, no. 7553, pp. 467–475, 2015.

[2] C. Laschi, B. Mazzolai, and M. Cianchetti, "Soft robotics: Technologies and systems pushing the boundaries of robot abilities," *Science Robotics*, vol. 1, no. 1, 2016.

[3] J. Shintake, V. Cacucciolo, D. Floreano, and H. Shea, "Soft robotic grippers," *Advanced Materials*, vol. 30, no. 29, p. 1 707 035,

[4] M. Runciman, A. Darzi, and G. P. Mylonas, "Soft robotics in minimally invasive surgery," *Soft Robotics*, vol. 0, no. 0, null, 0, PMID: 30920355.

[5] P. Polygerinos, N. Correll, S. A. Morin, B. Mosadegh, C. D. Onal, K. Petersen, M. Cianchetti, M. T. Tolley, and R. F. Shepherd, "Soft Robotics: Review of Fluid-Driven Intrinsically Soft Devices; Manufacturing, Sensing, Control, and Applications in Human-Robot Interaction," *Advanced Engineering Materials*, vol. 19, no. 12, e201700016,

[6] M. Cianchetti, C. Laschi, A. Menciassi, and P. Dario, "Biomedical applications of soft robotics," *Nature Reviews Materials*, vol. 3, no. 6, pp. 143–153, 2018.

[7] T. George Thuruthel, Y. Ansari, E. Falotico, and C. Laschi, "Control strategies for soft robotic manipulators: A survey," *Soft Robotics*, vol. 5, no. 2, pp. 149–163, 2018.

[8] W. McMahan, B. A. Jones, and I. D. Walker, "Design and implementation of a multi-section continuum robot: Air-octor," in *2005 IEEE/RSJ International Conference on Intelligent Robots and Systems, IROS*, Aug. 2005, pp. 3345–3352.

[9] M. Calisti, M. Giorelli, G. Levy, B. Mazzolai, B. Hochner, C. Laschi, and P. Dario, "An octopus-bioinspired solution to movement and manipulation for soft robots," *Bioinspiration & Biomimetics*, vol. 6, no. 3, p. 36 002, 2011.

[10] I. S. Godage, G. A. Medrano-Cerda, D. T. Branson, E. Guglielmino, and D. G. Caldwell, "Dynamics for variable length multisection continuum arms," *The International Journal of Robotics Research*, vol. 35, no. 6, pp. 695–722, 2016.

[11] M. Cianchetti, T. Ranzani, G. Gerboni, I. D. Falco, C. Laschi, S. Member, and A. Menciassi, "STIFF-FLOP surgical manipulator: Mechanical design and experimental characterization of the single module," in *2013 IEEE/RSJ International Conference on Intelligent Robots and Systems*, Nov. 2013, pp. 3576–3581.

[12] P. H. Nguyen, C. Sparks, S. G. Nuthi, N. M. Vale, and P. Polygerinos, "Soft Poly-Limbs: Toward a New Paradigm of Mobile Manipulation for Daily Living Tasks," *Soft Robotics*, soro.2018.0065, 2018.

[13] A. D. Marchese and D. Rus, "Design, kinematics, and control of a soft spatial fluidic elastomer manipulator," *The International Journal of Robotics Research*, vol. 35, no. 7, pp. 0 278 364 915 587 925–, 2015.

[14] T. Liu, Y. Wang, and K. Lee, "Three-dimensional printable origami twisted tower: Design, fabrication, and robot embodiment," *IEEE Robotics and Automation Letters*, vol. 3, no. 1, pp. 116–123, Jan. 2018.

[15] S.-J. Kim, D.-Y. Lee, G.-P. Jung, and K.-J. Cho, "An origami-inspired, self-locking robotic arm that can be folded flat," *Science Robotics*, vol. 3, no. 16, 2018.

[16] C. M. Best, M. T. Gillespie, P. Hyatt, L. Rupert, V. Sherrod, and M. D. Killpack, "A new soft robot control method: Using model predictive control for a pneumatically actuated humanoid," *IEEE Robotics Automation Magazine*, vol. 23, no. 3, pp. 75–84, Sep. 2016.

[17] P. H. Nguyen, I. B. Imran Mohd, C. Sparks, F. L. Arellano, W. Zhang, and P. Polygerinos, "Fabric soft poly-limbs for physical assistance of daily living tasks," in *2019 International Conference on Robotics and Automation (ICRA)*, May 2019, pp. 8429–8435.

[18] X. Liang, H. Cheong, Y. Sun, J. Guo, C. K. Chui, and C. Yeow, "Design , Characterization and Implementation of a Two - DOF Fabric - based Soft Robotic Arm," *IEEE Robotics and Automation Letters*, vol. 3766, no. c, pp. 1–8, Jul. 2018.

[19] M. A. Robertson and J. Paik, "New soft robots really suck: Vacuum-powered systems empower diverse capabilities," *Science Robotics*, vol. 2, no. 9, 2017.

[20] M. Wehner, M. T. Tolley, Y. Mengüç, Y.-L. Park, A. Mozeika, Y. Ding, C. Onal, R. F. Shepherd, G. M. Whitesides, and R. J. Wood, "Pneumatic energy sources for autonomous and wearable soft robotics," *Soft robotics*, vol. 1, no. 4, pp. 263–274, 2014.

[21] D. P. Holland, C. Abah, M. Velasco-Enriquez, M. Herman, G. J. Bennett, E. A. Vela, and C. J. Walsh, "The soft robotics toolkit: Strategies for overcoming obstacles to the wide dissemination of soft-robotic hardware," *IEEE Robotics Automation Magazine*, vol. 24, no. 1, pp. 57–64, Mar. 2017.

[22] H. Wang, M. Totaro, and L. Beccai, "Toward perceptive soft robots: Progress and challenges," *Advanced Science*, vol. 5, no. 9, p. 1 800 541, 2018.

[23] B. Shih, D. Drotman, C. Christianson, Z. Huo, R. White, H. I. Christensen, and M. T. Tolley, "Custom soft robotic gripper sensor skins for haptic object visualization," in *2017 IEEE/RSJ International Conference on Intelligent Robots and Systems (IROS)*, Sep. 2017, pp. 494–501.

[24] H. A. Wurdemann, S. Sareh, A. Shafti, Y. Noh, A. Faragasso, D. S. Chathuranga, H. Liu, S. Hirai, and K. Althoefer, "Embedded electroconductive yarn for shape sensing of soft robotic manipulators," in *2015 37th Annual International Conference of the IEEE Engineering in Medicine and Biology Society (EMBC)*, Aug. 2015, pp. 8026–8029.

[25] P. A. Xu, A. K. Mishra, H. Bai, C. A. Aubin, L. Zullo, and R. F. Shepherd, "Optical lace for synthetic afferent neural networks," *Science Robotics*, vol. 4, no. 34, 2019.

[26] M. C. Yuen, T. R. Lear, H. Tonoyan, M. Telleria, and R. Kramer-Bottiglio, "Toward closed-loop control of pneumatic grippers during pack-and-deploy operations," *IEEE Robotics and Automation Letters*, vol. 3, no. 3, pp. 1402–1409, Jul. 2018.

[27] R. L. Truby, R. K. Katzschmann, J. A. Lewis, and D. Rus, "Soft robotic fingers with embedded ionogel sensors and discrete actuation modes for somatosensitive manipulation," in *2019 2nd IEEE International Conference on Soft Robotics (RoboSoft)*, Apr. 2019, pp. 322–329.

[28] P. H. Nguyen, F. Lopez-Arellano, W. Zhang, and P. Polygerinos, "Design, characterization, and mechanical programming of fabric-reinforced textile actuators for a soft robotic hand," in *2019 IEEE/RSJ International Conference on Intelligent Robots and Systems (IROS)*, Nov. 2019, pp. 8312–8317.

[29] R. J. Webster, B. a. Jones, R. J. W. Iii, B. a. Jones, I. I. I. Robert J. Webster, and B. a. Jones, "Design and Kinematic Modeling of Constant Curvature Continuum Robots: A Review," *The International Journal of Robotics Research*, vol. 29, no. 13, pp. 1661–1683, 2010.

[30] A. Liang, R. Stewart, and N. Bryan-Kinns, "Analysis of sensitivity, linearity, hysteresis, responsiveness, and fatigue of textile knit stretch sensors," *Sensors*, vol. 19, no. 16, p. 3618, Aug. 2019.